Manufacturing Letters 31 (2022) 69–73

Contents lists available at ScienceDirect

Manufacturing Letters

journal homepage: www.elsevier.com/locate/mfglet

# Calibration uncertainty in nanoparticle sintering simulations

Obehi G. Dibua [a], Chee S. Foong [b], Michael Cullinan [a]

[a] Department of Mechanical Engineering, University of Texas at Austin, Austin, TX 78712, United States
[b] NXP Semiconductors, Austin, TX 78735, United States

ARTICLE INFO

*Article history:*
Received 26 February 2021
Received in revised form 30 May 2021
Accepted 6 July 2021
Available online 22 July 2021

*Keywords:*
Simulation
Calibration
Uncertainty Quantification
Nanoparticle Sintering
Phase Field Modelling
Modelling Particle Beds

ABSTRACT

Previous papers have demonstrated how nanoparticles in the Microscale Selective Laser Sintering process densify under conditions of isothermal heating, yielding a time calibration factor which relates the predicted sintering time to simulation time. However, it is important to quantify the uncertainty related to the time calibration factor in order to state with any degree of confidence the sintering window during which the physical process can be expected to achieve the degree of sintering predicted by the simulation. As such, the goal of this paper is to quantify the uncertainty related to the time calibration factor.


## 1. Introduction

Commercially available Additive Manufacturing (AM) processes generally have minimum features sizes on the order of hundreds of micrometers [1,2]. This resolution limitation prohibits industries, where sub-10 μm parts are desired, from benefitting from the unique advantages available with AM. Microscale Selective Laser Sintering (μ-SLS) is a process that has been created to mitigate these resolution issues in metal AM parts [3–5]. In μ-SLS a layer of nanoparticle ink is deposited onto a substrate. Then a laser is directed off a micromirror array which projects a sintering pattern onto the nanoparticles with microscale resolution [3–5].

A simulation for the nanoparticle sintering in this μ-SLS process has been presented previously by the authors [6,7]. This simulation uses Phase Field Modelling (PFM) to study the densification rate associated with nanoparticles undergoing sintering. The simulations in [6] yield densification curves for a one-by-one micrometer bed calibrated to isothermal heating at 450 °C, 500 °C, and 550 °C. The result of this calibration was a single value for the time calibration factor. However, this single value does not account for the uncertainties associated with the calibration. There are two major sources of uncertainty associated with these calibrations. The first source of uncertainty is a result of the uncertainty inherent in the experimentation process [6], and the second comes from the randomness in the arrangement of particles in the bed generation procedure [8,9].

To derive the total uncertainty, several random nanoparticle beds are generated and sintered. The uncertainty from these random beds is then propagated through the uncertainty from the experiments. This process yields the uncertainty in the time calibration factor, which maps simulation timesteps to time in seconds. Uncertainty in the time calibration factor gives the window of time for which the actual system could be expected to achieve the sintering extent predicted by the simulation.

## 2. Results and discussion

### 2.1. Single temperature single curve fit

The uncertainty analysis was carried out on thirteen two-by-two micrometer beds that were randomly generated and consist of particles with diameters between 4 and 40 pixels. The size calibration value for these simulations was 10.584 nm/pixel. This range of diameters was chosen to match that of the copper nanoparticles being modelled, which were experimentally measured to have a diameter with a 95% Confidence Interval between 40 and 424 nm [10]. Of the thirteen beds generated, the first nine beds were generated as two-by-two micrometer beds with identical bed generation parameters, while the last four beds were two two-by-two beds extracted from the center of beds generated as four-by-four micrometer beds and two two-by-two beds generated with more mixing. The four-by-four micrometer beds were incor-

https://doi.org/10.1016/j.mfglet.2021.07.010

porated into the study to determine the effect that boundary conditions may have on the results.

Starting with the initial beds generated, the sintering simulation and analysis follows a procedure graphically outlined in Fig. 1 [6]. The particles in the beds undergo sintering starting from the state in Fig. 1a until a final sintering extent shown in 1b is reached. Then densification curves similar to that in 1c, obtained from analysis done on 95 pixels$^2$ boxes in the center of the two-by-two micrometer simulation beds, were calibrated to the experimental data curve in 1d and the time calibration factor $A$ was derived. $A$ is the map of simulation timesteps to time in microseconds as defined in Eq. (1). The value $A$ was chosen as the one that minimizes the error between the experimental data and simulation data as in 1e. This process was carried out for all thirteen beds.

$$A = \frac{Actual\ time(\mu s)}{Number\ of\ simulation\ timesteps} \quad (1)$$

The calibration process gave an average $A$ value of 22.3 ± 3.6 μs/timestep for the nine beds generated the same way. The two beds extracted from the center of the four-by-four

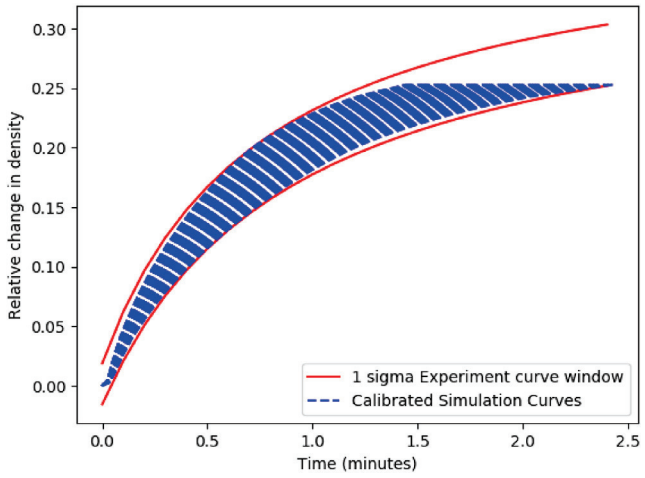


**Fig. 2.** 550 °C Sintering Calibration to an Uncertainty Band.

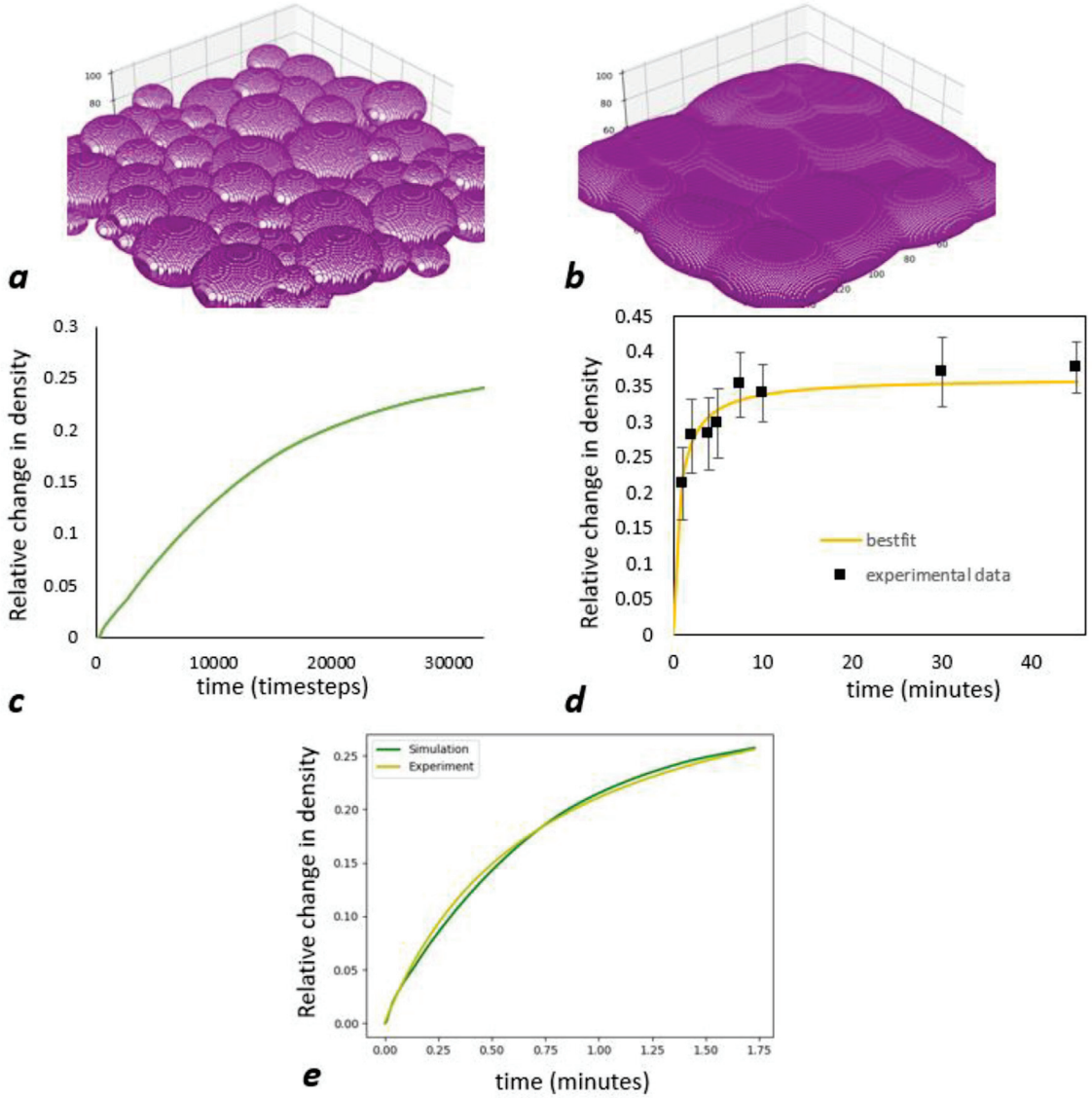


**Fig. 1.** (a) Initial unsintered bed, (b) Final sintered bed, (c) Density curve extracted from an analysis of the sintering simulation, (d) Experimental data curve fit for sintering at 550 °C, (e) Simulation calibration fit to experiment.

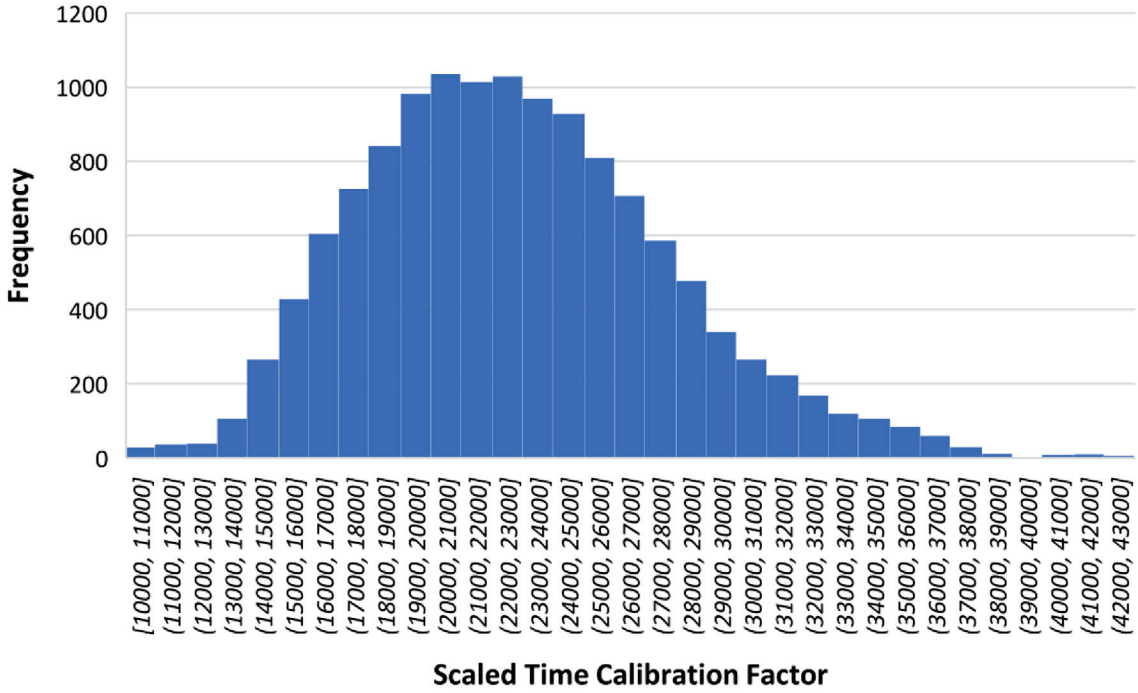


(a)

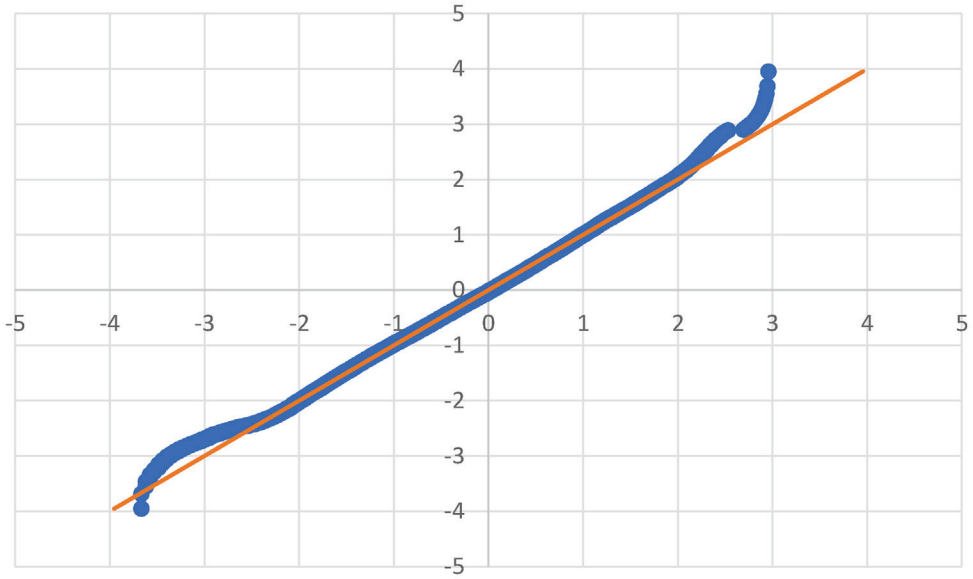


(b)

**Fig. 3.** (a) Histogram of all the scaled time calibration values, *A/100*, collated from the analysis done on all randomly generated beds and fit to the uncertainty band for the 550 °C experiment (b) Q-Q plot to verify normal distribution of the natural log of the data in Fig. 3a. A Q-Q plot is a plot of two sets of quantiles against each other to determine if they are both of the same distribution. If the plot gives a straight line, then they are of the same distribution. In this plot the natural log of the data is compared to a normal distribution and the straightness of the scatter plot shows that the natural log does indeed follow a normal distribution, which means that the original data is confirmed to follow a lognormal distribution.

micrometer beds, as well as the two beds created with different restitution coefficients, gave *A* values which fall between a 95% confidence interval of the mean and standard deviation derived from the first nine beds. Since all four *A* values from beds created with different bed generation parameters fall within the uncertainty from the nine beds all created with the same parameters, the conclusion can be made that the uncertainty resulting from the parameters used in generating the beds is small compared to the inherent uncertainty resulting from the differences in the arrangement of nanoparticles within the beds themselves.

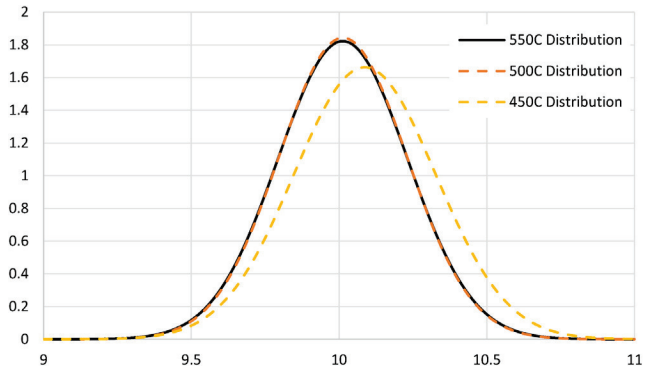


**Fig. 4.** Comparison of the normal log of time calibration distributions for different temperatures.

### 2.2. Single temperature uncertainty band

The results above do not incorporate the uncertainty associated with the experimentation process. For sintering experiments done on copper nanoparticles at 550 °C, the associated uncertainty is shown in Fig. 1d. Several exponential fits can be derived from the experiment curves in Fig. 1d which would satisfactorily fall within the uncertainties. As such, it would be inaccurate to solely obtain time calibration data from a single curve fit to a single set of points on any one curve. To obtain a full measure of the uncertainty associated with the process, calibration is done to all curve fits within a band defined by the uncertainty of the experiments. First, several *A* values are chosen, then the densification curves are calibrated using these *A* values and the calibrated simulation curves are fit within the uncertainty bands from the experiments. With this method, all possible *A* values that result in simulation calibrations within the acceptable limits for the experiment are determined. An example is shown in Fig. 2, where the blue dashes are the calibrated simulation curves, and the red lines represent the uncertainty window for the experimental results.

The process of fitting the simulation data to uncertainty bands was carried out for all the analysis boxes. *A* values were determined from the calibration process and Fig. 3a shows the final histogram derived from the collation of the analysis done. This data includes all *A* values calibrating to curves within the uncertainty bands for each of the eighteen analysis boxes taken from all thirteen generated beds. The histogram, in Fig. 3a, and q-q plot, in Fig. 3b, show the *A* values most closely follow a lognormal distribution. A Kolmogorov Smirnov test [11] performed on the hypothesis of a lognormal distribution, yielded a p-value of 0.42, further validating the lognormal distribution assumption. The mean of the overall distribution is 27.5 μs/timestep with a standard deviation of 6.1 μs/timestep. Comparing these overall results to the results derived from examining a single curve fit shows that the random arrangement of particles in the bed contributes a larger amount to the overall uncertainty, but that it is still necessary to account for the contribution from the uncertainty in the initial temperature curves in the overall uncertainty for the time calibration factor.

### 2.3. Other temperatures

The procedure outlined for calibrating to sintering at 550 °C was repeated for experiments done at 450 °C and 500 °C, for a single bed. The expectation from this study is that the *A* value derived from calibrating to these temperatures should fall within the distribution in Fig. 3a. This should be the case because *A* should be independent of the temperature that the simulation is being calibrated to. Once the *A* value distributions for these new temperatures were obtained, the distributions were compared to that in Fig. 3a, and the result is shown in Fig. 4. The log of the data values was used for these comparisons to make it easier to compare them as normal distributions. A z-test was used to determine how close the means of the 500 °C and 450 °C distributions are to that of the 550 °C distribution. A z-value of 0.341 was found when comparing the 550 °C and 450 °C distributions, and 0.003 was found for the comparison between 500 °C and 550 °C. These values show that the means for the 450 °C and 500 °C distributions are within 1 standard deviation of the 550 °C distribution.

## 3. Conclusion

This paper demonstrates an approach to quantifying the total uncertainty associated with the calibration of simulation time to sintering time for a nanoparticle sintering simulation. Comparing the amounts of uncertainty related to generating the simulation beds with the uncertainties created by the inherent randomness of the particle locations in the bed showed that the largest source of uncertainty comes from the random arrangement of particles in the simulation beds. This has implications on the bed generation process for the sintering simulations run. It shows that for future analysis performed with these simulations the bed generation can be carried out with varying generation parameters without impact on the final distribution of the results. Also, comparing the calibration results from one temperature to those done on other temperatures revealed that changing the temperature had no statistically significant change on the time calibration factor. This means that the simulation is robust enough to handle this change in temperature without changing the result derived. Consequently, future analysis for such temperature independent properties need only be performed on simulation beds sintered to a single temperature. It is worth noting that the results presented here are dependent on the material and size distribution of the particles under study. Additionally, further testing is required to understand what effect sintering between nanoparticle layers has on these results.

## Declaration of Competing Interest

The authors declare that they have no known competing financial interests or personal relationships that could have appeared to influence the work reported in this paper.

## Acknowledgements

This study was made possible through the Supercomputing resources of the Texas Advanced Computing Center, and support from NXP Semiconductors. This material is based upon work supported by the National Science Foundation under Grant No. 1728313.

## References

[1] Design Guidelines: Laser Sintering (LS), (n.d.). Retrieved June 28, 2017, from https://www.stratasysdirect.com/resources/laser-sintering/.
[2] B. Sager, D. Rosen, Stereolithography Process Resolution, Georgia Institute of Technology, (n.d.).
[3] Roy NK, Foong CS, Cullinan MA. Design of a Micro-scale Selective Laser Sintering System. 2016 Annual International Solid Freeform Fabrication Symposium, 2016.
[4] N. Roy, A. Yuksel, M. Cullinan, Design and Modeling of a Microscale Selective Laser Sintering System, ASME 2016 11th International Manufacturing Science and Engineering Conference, (2016).
[5] Roy N, Dibua O, Foong CS, Cullinan M. Preliminary Results on the Fabrication of Interconnect Structures Using Microscale Selective Laser Sintering. Proceedings of the ASME 2017 International Technical Conference and Exhibition on Packaging and Integration of Electronic and Photonic Microsystems, 2017.

[6] Dibua O, Yuksel A, Roy N, Foong CS, Cullinan M. Nanoparticle sintering model: simulation and calibration against experimental data. J Micro- Nano-Manuf 2018;6:041004-1–0414004-9.
[7] Dibua O, Yuksel A, Roy N, Foong CS, Cullinan M. Nanoparticle, modelling nanoparticle sintering in a microscale selective laser sintering process. In: Proceedings of the 28th Annual International Solid Freeform Fabrication Symposium. p. 1018–29.
[8] R. Garg, J. Galvin, T. Li, S. Pannala, Documentation of open-source MFIX-DEM software for gas-solids flows, (2012).
[9] Yuksel A, Cullinan M. Modeling of nanoparticle agglomeration and powder bed formation in microscale selective laser sintering systems. Addit Manuf 2016;12:204–15.
[10] Roy N, Foong CS, Cullinan M. Effect of size, morphology, and synthesis method on the thermal and sintering properties of copper nanoparticles for use in microscale additive manufacturing processes. Addit Manuf 2018;21:17–29.
[11] Hodges Jr JL. The significance probability of the smirnov two-sample test. Arkiv fiur Matematik 1958;3(43):469–86.